Discontinuous transition to synchrony in the Kuramoto-Sakaguchi model with a uniform distribution of frequencies

A. Pikovsky [*]
Department of Physics and Astronomy, University of Potsdam, Karl-Liebknecht-Straße 24/25, 14476 Potsdam-Golm, Germany

(Received 12 April 2026; revised 16 May 2026; accepted 20 May 2026; published 28 May 2026)

The transition to synchrony in the Kuramoto model of globally coupled phase oscillators with a uniform distribution of natural frequencies is discontinuous. We extend the theory of this transition to the Kuramoto-Sakaguchi model, taking into account a phase shift in coupling. In the thermodynamic limit, we derive dependencies of the order parameters on the coupling strength and the phase shift, and describe two transitions from disorder to partial synchrony and from partial synchrony to complete synchrony. In all cases, the first transition is discontinuous, although for phase shifts close to $\pi/2$, the jump is exponentially small. We also discuss which properties of the transition hold for distributions close to the uniform one.

DOI: 10.1103/lfvq-b68c

I. INTRODUCTION

Onset of synchronization in a large population of coupled oscillators can be considered as a nonequilibrium disorder-order phase transition [1]. As the order parameter, one can use the amplitude of the collective oscillating mode, which vanishes in the disordered state. In a deterministic setup, disorder in the natural frequency of the units plays the role of temperature, and an attractive coupling between oscillators should be strong enough for synchronization to appear. In 1975, Y. Kuramoto proposed his paradigmatic model of globally coupled phase oscillators to explain this phenomenon and presented a self-consistent theory of the transition [2,3]. For different extensions of this approach, see Ref. [4].

In the standard Kuramoto setup, the transition to synchrony can be characterized by the order parameter, defined as a complex mean field [see Eq. (2)]. This order parameter is well defined in the thermodynamic limit, where the theory is formulated, and vanishes in the disordered phase. At a critical coupling, the amplitude of the order parameter grows as a square root of the parameter variation, resembling a supercritical Hopf bifurcation [5]. In experiments, where the number of units in an ensemble is finite (e.g., 64 chemical oscillators in Ref. [6] and 72 electronic oscillators in Ref. [7]), the order parameter does not vanish in the disordered phase, and thus the transition is smeared. For finite ensembles, for a strong enough coupling, one observes a second transition to complete locking, where all oscillators have the same frequency [7]. While finite-size effects are an important topic of current research, we focus in this paper on the thermodynamic limit of an infinite ensemble, where one follows not individual oscillators but densities.

[*]Contact author: pikovsky@uni-potsdam.de

Published by the American Physical Society under the terms of the Creative Commons Attribution 4.0 International license. Further distribution of this work must maintain attribution to the author(s) and the published article's title, journal citation, and DOI.

There are several factors that modify the standard Kuramoto picture in the thermodynamic limit of large ensembles. For example, the nature of the transition is sensitive to the shape of the coupling function: An addition of a small-amplitude second harmonics to the coupling can transform the supercritical transition to a first-order one with a hysteresis or to a transcritical transition [8–10]. Even for a purely sin-coupling, as adopted by Kuramoto, the nature of the transition, i.e., whether it is continuous or discontinuous, heavily depends on the distribution of the natural frequencies of the oscillators. An important special case is the uniform distribution of frequencies. In a seminal paper [11], D. Pazó has shown that the Kuramoto model with a uniform distribution of the frequencies demonstrates, in the thermodynamic limit, a discontinuous transition without hysteresis. Since then, the case of uniform distribution attracted large interest [12–15].

In this paper, we explore synchronization transition for a uniform distribution of natural frequencies in the Kuramoto-Sakaguchi model [16], which is an extension of the Kuramoto model for the case of an additional phase shift α in the coupling [see Eq. (1)]. This phase shift allows for a continuous shift from attractive ($\cos\alpha > 0$) to repulsive ($\cos\alpha < 0$) coupling, with a conservative coupling ($\alpha = \pm\pi/2$) at the border of attraction and repulsion. One could expect that because coupling is maximally attracting in the Kuramoto case of vanishing α, the critical coupling constant grows as one approaches the border of attraction. Indeed, in the case of Cauchy distribution of natural frequencies, one can show analytically [17] that the critical coupling diverges $\sim(\cos\alpha)^{-1}$. Interestingly, in the case of a uniform distribution discussed below, the threshold of synchronization *decreases* with the parameter of the phase shift $\sim\cos\alpha$. We note here that the phase shift in the coupling α typically appears for ensembles of oscillating units coupled via a common load, response of which is phase shifted with regard to the forcing (*LCR* load for electronic oscillators [7] and Josephson junctions [18], common support for clocks and metronomes [19]).

The paper is organized as follows. We introduce the model and describe the phenomenology of the synchronization transition in Sec. II. In our analysis, we use the method developed by Omel'chenko and Wolfrum in Refs. [20,21]; we describe it in Sec. III. In Sec. IV, we present the derivation of the main results. Stability is discussed in Sec. V. In Sec. VI, we provide a qualitative interpretation of the analytic results and show which of them are valid also for distributions close to the uniform one. We conclude with a discussion in Sec. VII.

II. DISCONTINUOUS TRANSITION IN THE KURAMOTO-SAKAGUCHI MODEL

The Kuramoto-Sakaguchi model [16] describes the dynamics of N phase oscillators with a mean-field coupling, and is formulated as a set of equations

$$\dot{\varphi}_k = \omega_k + \frac{\varepsilon}{N}\sum_j \sin(\varphi_j - \varphi_k - \alpha) = \omega_k + \varepsilon R\sin(\Psi - \varphi_k - \alpha). \tag{1}$$

Here, ω_k are oscillators' natural frequencies, which are taken from a distribution $g(\omega)$. Collective variables R and Ψ are, respectively, the amplitude and the argument of the complex mean field

$$Z = Re^{i\Psi} = \frac{1}{N}\sum_j e^{i\varphi}. \tag{2}$$

The system has two parameters, the phase shift α and the coupling strength ε. The case $\alpha = 0$ is the Kuramoto model [3].

Mutual attraction of the phases (which is ensured if $-\pi/2 < \alpha < \pi/2$) results in a synchronization transition, which is perfect in the thermodynamic limit $N \to \infty$. In this limit, in the asynchronous state $R = 0$, while $R > 0$ indicates some synchrony in the population; thus, R has been picked by Kuramoto as the order parameter of the nonequilibrium synchrony-asynchrony transition. The nature of the transition heavily depends on the distribution $g(\omega)$. For a one-humped distribution with a single smooth maximum, typically a simple second-order continuous transition is observed (see, however, more complex situations for nontrivial distributions in Refs. [20,21]), while for two-humped distributions a first-order transition with a hysteresis is typical.

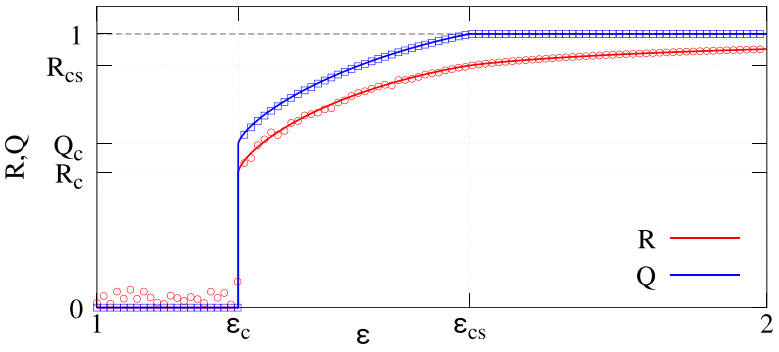


FIG. 1. Lines: Typical dependence of the order parameter R and of the fraction of locked oscillators Q on the coupling strength ε (here drawn for $\alpha = \pi/10$ according to exact expressions derived below). At ε_c, both characteristics jump to values R_c and Q_c, demonstrating a discontinuous transition to synchrony. At ε_{cs}, the value of Q reaches its maximal value 1, which marks a transition to complete synchrony. Symbols: Results of numerical simulations with $N = 1000$.

An interesting intermediate case for the Kuramoto model happens for a uniform distribution of frequencies: Here, a discontinuous transition to synchrony occurs [11]. The goal of this paper is to extend the results of Ref. [11] to the Kuramoto-Sakaguchi model. Remarkably, all relevant quantities can be calculated analytically in the thermodynamic limit. Before proceeding with the theory, we describe the phenomenology of the synchronization transition and define its main characteristics.

Typically, one is interested in the dependence of the order parameter R on the coupling strength ε at a fixed phase shift parameter α. We show this dependence in Fig. 1. At ε_c, there is a discontinuous transition from 0 to R_c; for larger couplings, R grows monotonically with ε. In this figure, we also show another characteristic of the synchronization transition, the fraction of locked oscillators Q. If the mean-field amplitude R is nonzero, some oscillators are locked by the mean field (and are also mutually locked), while others have frequencies different from that of the mean field. At the transition point ε_c, this fraction also experiences a jump from zero to some value Q_c. Further growth of Q leads to another transition at ε_{cs}, above which $Q = 1$, which means that all units are mutually locked and the dynamics of the ensemble is purely periodic (complete synchrony). Note that R is still <1 here because the phase distribution is not a delta function.

In Fig. 1, we also illustrate how the two transitions look in numerical simulations with a finite ensemble. Below critical coupling, the average order parameter $\langle R \rangle$ is nonzero due to finite-size fluctuations, while $Q = 0$. In the simulations, we varied the coupling parameter in steps of $\Delta\varepsilon = 0.01$, and at this resolution, the synchronization transition appears discontinuous. Behavior of the simulated order parameters at $\varepsilon > \varepsilon_c$ follows the theoretical prediction in the thermodynamic limit quite well.

The two critical values of coupling strength, ε_c and ε_{cs}, depend on the phase shift parameter α, as it is shown in Fig. 2. Note that for $\alpha = 0$, $\varepsilon_c = \varepsilon_{cs}$, in accordance with results of Ref. [11]. Figure 2 can be considered as the full diagram of possible regimes for the model under consideration; the borders are derived analytically in Sec. IV.

Finally, in Fig. 3, we show dependencies of R_c, R_{cs}, and Q_c on α. One can see that the jumps R_c and Q_c drastically decrease with α, but they are finite in the whole range $0 \leqslant \alpha < \pi/2$, to be discussed in detail in Sec. IV D.

III. SELF-CONSISTENT ANALYSIS OF THE SYNCHRONOUS STATE

In our analysis, we will follow the approach developed in Refs. [20,21]. For the sake of consistency, we will succinctly present it here.

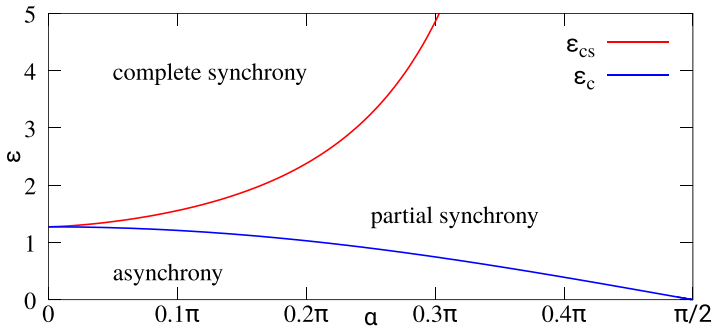


FIG. 2. Dependence of the two critical values of coupling strength, ε_c and ε_{cs}, on the parameter α.

A. Generic case

In the thermodynamic limit, we denote oscillators with natural frequency ω as φ_ω and rewrite Eqs. (1) and (2) as

$$\dot{\varphi}_\omega = \omega + \varepsilon R \sin(\Psi - \varphi_\omega - \alpha), \quad Re^{i\Psi} = \langle e^{i\varphi} \rangle = \int d\omega\, g(\omega) \int d\varphi\, \rho(\varphi|\omega) e^{i\varphi}. \tag{3}$$

Here, $\rho(\varphi|\omega)$ is the density of oscillators with natural frequency ω.

One looks for a periodic in time (statistically stationary) solution where $R = \text{const}$ and the phase of the mean field rotates with a constant (still unknown) frequency Ω: $\Psi = \Omega t + \Psi_0$. It is convenient to make a transformation to the rotating reference frame, where the right-hand side will be time independent:

$$\varphi = \vartheta + \Psi - \alpha = \vartheta + \Omega t + \Psi_0 - \alpha.$$

The physical meaning of the new phase ϑ is the phase shift with regard to the uniformly rotating phase of the mean field. Then, Eq. (3) is rewritten in terms of ϑ as

$$\dot{\vartheta}_\omega = \omega - \Omega - \varepsilon R \sin \vartheta_\omega, \quad Re^{i\alpha} = \langle e^{i\vartheta} \rangle = \int d\omega\, g(\omega) \int d\vartheta\, \rho(\vartheta|\omega) e^{i\vartheta}. \tag{4}$$

The next step is to find the stationary distribution $\rho(\vartheta|\omega)$ and the integral $\int d\vartheta\, \rho(\vartheta|\omega) e^{i\vartheta}$. Let us denote

$$s = \frac{\omega - \Omega}{\varepsilon R} \tag{5}$$

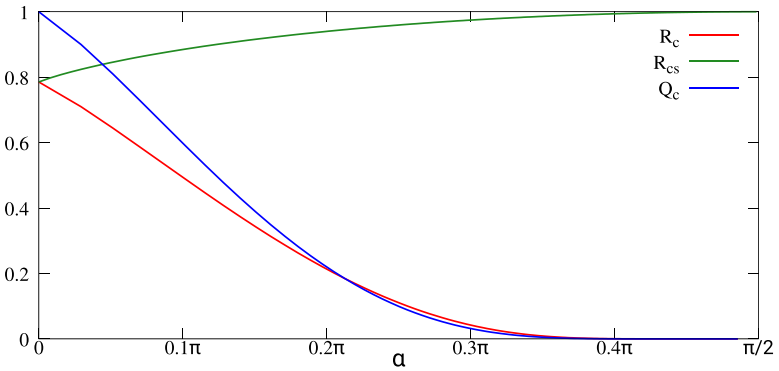


FIG. 3. Dependencies of the steps R_c and Q_c on the parameter α. Additionally, the value R_{cs} (also indicated in Fig. 1) of the order parameter R at the transition to complete synchrony is shown.

and rewrite Eq. (4) as

$$\dot{\vartheta}_\omega = \varepsilon R(s - \sin\vartheta_\omega). \tag{6}$$

In this equation, the factor εR defines the timescale and is irrelevant for the stationary invariant distribution of the phase; the latter depends on the parameter s only.

The dynamics of Eq. (6) is as follows: (1) For $|s| < 1$, there is a stable steady state $\vartheta = \arcsin(s)$; and (2) for $|s| > 1$, the phase rotates, and its distribution density is inversely proportional to the velocity of the motion $\sim|s - \sin\vartheta|^{-1}$. This yields

$$\rho(\vartheta|\omega) = \begin{cases} \delta(\vartheta - \arcsin(s)), & \text{for } |s| \leqslant 1, \\ \frac{\sqrt{s^2-1}}{2\pi}\frac{1}{|s-\sin\vartheta|}, & \text{for } |s| > 1. \end{cases} \tag{7}$$

This allows for calculation of the integral in Eq. (4) as follows:

$$\int d\vartheta\ \rho(\vartheta|\omega)e^{i\vartheta} = h(s) = \begin{cases} is(1 - \sqrt{1 - s^{-2}}), & \text{for } |s| > 1, \\ is + \sqrt{1 - s^2}, & \text{for } |s| \leqslant 1. \end{cases} \tag{8}$$

Substitution of this integral in Eq. (4) yields the following relation:

$$Re^{i\alpha} = \int d\omega\, g(\omega)h\left(\frac{\omega - \Omega}{\varepsilon R}\right) = \varepsilon R \int ds\, g(\Omega + \varepsilon Rs)h(s), \tag{9}$$

which has the meaning of a complex self-consistency equation defining the synchronous state.

Let us introduce parameter $A = \varepsilon R$ and complex-valued function $f(\Omega, A)$ as

$$f(\Omega, A) = \int ds\, g(\Omega + As)h(s). \tag{10}$$

With this function, we can find from Eq. (9) the parameters α and ε as functions of Ω and A:

$$R = A|f(\Omega, A)|, \quad \varepsilon = \frac{1}{|f(\Omega, A)|}, \quad \alpha = \arg f(\Omega, A). \tag{11}$$

This provides a solution to the problem, namely, the dependence of the order parameter R on the coupling constant ε, in a parametric form.

Additionally, from Eq. (8), one can find which oscillators are locked to the mean field and which are rotating with respect to the mean field: The locked oscillators have natural frequencies in the interval $\Omega - A \leqslant \omega \leqslant \Omega + A$; the rotating oscillators have natural frequencies outside of this interval. Thus, the fraction of locked units Q is calculated as

$$Q = \int_{\Omega-A}^{\Omega+A} d\omega\ g(\omega). \tag{12}$$

Summarizing, all the quantities of interest are represented in the parametric form via the integrals over the distribution of natural frequencies:

$$R = A|f(\Omega, A)|, \tag{13}$$

$$\varepsilon = \frac{1}{|f(\Omega, A)|}, \tag{14}$$

$$\alpha = \arg f(\Omega, A), \tag{15}$$

$$Q = \int_{\Omega-A}^{\Omega+A} d\omega\ g(\omega), \tag{16}$$

$$f(\Omega, A) = \int ds\, g(\Omega + As)h(s). \tag{17}$$

B. Kuramoto model, uniform distribution of frequencies

We first apply expressions (13)–(17) to the Kuramoto model and reproduce results of Ref. [11]. In the Kuramoto model, $\alpha = 0$. If $g(\omega)$ is an even function, then due to symmetry we set $\Omega = 0$ and obtain

$$f(0, A) = \int_{-1}^{1} g(Ay)\sqrt{1 - y^2}\, dy. \tag{18}$$

[Here, only the even part of $h(s)$ contributes.] For a uniform distribution,

$$g(\omega) = \begin{cases} \frac{1}{2}, & |\omega| < 1, \\ 0, & |\omega| > 1, \end{cases} \tag{19}$$

we obtain

$$f(0, A) = \begin{cases} \frac{\pi}{4}, & A \leqslant 1, \\ \frac{1}{2}\left[\frac{1}{A}\sqrt{1 - \left(\frac{1}{A}\right)^2} + \arcsin\frac{1}{A}\right], & A > 1 \end{cases} \tag{20}$$

and

$$Q = \begin{cases} A, & A \leqslant 1, \\ 1, & A > 1. \end{cases} \tag{21}$$

This yields the $R(\varepsilon)$ dependence in a parametric form:

$$R = Af(0, A), \quad \varepsilon = \frac{1}{f(0, A)}. \tag{22}$$

At $\varepsilon_c = 4/\pi$, the order parameter R takes values $0 \leqslant R \leqslant \pi/4$, which corresponds to a jump of the order parameter; further, at $\varepsilon > \varepsilon_c$, R grows. At ε_c, the value of Q is between $0 \leqslant Q \leqslant 1$, and for $\varepsilon > \varepsilon_c$ one has complete synchrony $Q = 1$. The transition to synchrony is discontinuous: At ε_c, the values of R and Q jump to $R_c = \pi/4$ and $Q_c = 1$, respectively; for $\varepsilon > \varepsilon_c$, the order parameter R grows and tends to 1 as $\varepsilon \to \infty$.

IV. KURAMOTO-SAKAGUCHI CASE, UNIFORM DISTRIBUTION OF FREQUENCIES

Here, we consider a general Kuramoto-Sakaguchi case $\alpha \neq 0$ for the uniform distribution (19). Because the distribution of frequencies is symmetric $g(-\omega) = g(\omega)$, the full system has a symmetry $\varphi \to -\varphi, \alpha \to -\alpha$. Thus, we restrict ourselves below to the case $\alpha > 0$; the solution for negative α can be obtained by setting $\Omega \to -\Omega$.

A. Analytic representation of the fraction of locked units

The simplest calculation is that of the fraction of synchronous oscillators Q. According to Eq. (16), for the uniform distribution of frequencies (19) we have

$$Q = \tfrac{1}{2}(\min(\Omega + A, 1) - \max(\Omega - A, -1)). \tag{23}$$

This leads to the following representation of the quantity Q:

$$Q = \begin{cases} A, & A < 1 - \Omega \quad \text{and} \quad A < 1 + \Omega, \\ \frac{1+\Omega+A}{2}, & 1 + \Omega < A < 1 - \Omega, \\ \frac{1+A-\Omega}{2}, & 1 - \Omega < A < 1 + \Omega, \\ 1, & A > 1 - \Omega \quad \text{and} \quad A > 1 + \Omega. \end{cases} \tag{24}$$

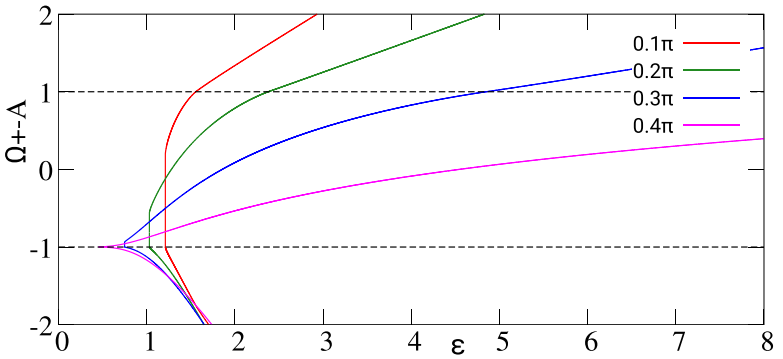


FIG. 4. The range of locked oscillators within the domain $-1 \leqslant \omega \leqslant 1$ (the domain is shown with dashed black lines), for different values of parameter α.

For convenience, we illustrate relations (23) and (24) in Fig. 4. Here, we plot values of $\Omega \pm A$ (the range where oscillators are locked to the mean field) versus coupling strength ε, for several values of the parameter α. We also show the range of natural frequencies $-1 \leqslant \omega \leqslant 1$. At ε_c, there is a step, and a finite portion of oscillators (with frequencies in the interval $-1 \leqslant \omega \leqslant 2Q-1$) become locked. This portion grows, and the second transition at ε_{cs} is where the upper branch of the curve crosses $\omega = 1$.

B. Analytic representations of function f

Let us calculate function $f(\Omega, A)$ [Eq. (17)] in the case of a uniform distribution (19):

$$f(\Omega, A) = \int ds\, g(\Omega + As)h(s) = \frac{1}{2}\int_{-(1+\Omega)/A}^{(1-\Omega)/A} h(s)\, ds. \tag{25}$$

It is convenient to separate real and imaginary parts of $h(s)$ [Eq. (8)]:

$$h(s) = h_r(s) + ih_i(s), \tag{26}$$

$$h_r(s) = \begin{cases} 0, & |s| > 1, \\ \sqrt{1-s^2}, & |s| \leqslant 1, \end{cases} \tag{27}$$

$$h_i(s) = \begin{cases} s(1-\sqrt{1-s^{-2}}), & |s| > 1, \\ s, & |s| \leqslant 1. \end{cases} \tag{28}$$

Taking indefinite integrals of these expressions, we obtain the following functions (H_r, H_i):

$$H_r(x) = \int^x h_r(s)\, ds = \begin{cases} -\frac{\pi}{4}, & x < -1, \\ \frac{1}{2}(\arcsin x + x\sqrt{1-x^2}), & -1 \leqslant x \leqslant 1, \\ \frac{\pi}{4}, & x > 1, \end{cases}$$

$$H_i(x) = \int^x h_r(s)\, ds = \begin{cases} \frac{x^2}{2}, & |x| \leqslant 1, \\ \frac{1}{4}\left[2x^2(1-\sqrt{1-x^{-2}}) + \ln\frac{1+\sqrt{1-x^{-2}}}{1-\sqrt{1-x^{-2}}}\right], & |x| > 1. \end{cases} \tag{29}$$

Substituting these functions in Eq. (25), we obtain an analytic expression of function f:

$$f(\Omega, A) = \frac{1}{2}\left[H_r\left(\frac{1-\Omega}{A}\right) - H_r\left(-\frac{1+\Omega}{A}\right)\right] + i\frac{1}{2}\left[H_i\left(\frac{1-\Omega}{A}\right) - H_i\left(-\frac{1+\Omega}{A}\right)\right]. \tag{30}$$

Below, we need to consider the limit as A approaches 0. For this purpose, it is convenient to represent the functions H_r and H_i from Eq. (29) as functions of $y = 1/x$.

For the real part, we have

$$G_r(y) = H_r\left(\frac{1}{y}\right) = \begin{cases} -\frac{\pi}{4}, & -1 < y < 0, \\ \frac{1}{2}(\arcsin(y^{-1}) + y^{-1}\sqrt{1-y^{-2}}), & |y| \geqslant 1, \\ \frac{\pi}{4}, & 0 < y < 1. \end{cases} \tag{31}$$

For the imaginary part, we have

$$G_i(y) = H_i\left(\frac{1}{y}\right) = \begin{cases} \frac{1}{2y^2}, & |y| \geqslant 1, \\ \frac{1}{4}\left[2y^{-2}(1-\sqrt{1-y^2}) + \ln\frac{1+\sqrt{1-y^2}}{1-\sqrt{1-y^2}}\right], & |y| \leqslant 1. \end{cases} \tag{32}$$

A slightly different equivalent form of G_i is obtained by multiplying and dividing by $1+\sqrt{1-y^2}$:

$$G_i(y) = \begin{cases} \frac{1}{2y^2}, & |y| > 1, \\ \frac{1}{2}\frac{1}{1+\sqrt{1-y^2}} + \frac{1}{4}\ln(2+2\sqrt{1-y^2}-y^2) & \\ -\frac{1}{2}\ln|y|, & |y| \leqslant 1. \end{cases} \tag{33}$$

In terms of these functions, the function f is represented as

$$f(\Omega, A) = \frac{1}{2}\left[G_r\left(\frac{A}{1-\Omega}\right) - G_r\left(-\frac{A}{1+\Omega}\right)\right] + i\frac{1}{2}\left[G_i\left(\frac{A}{1-\Omega}\right) - G_i\left(-\frac{A}{1+\Omega}\right)\right]. \tag{34}$$

The obtained expressions for the function f [Eqs. (30) and (34)] can be substituted in Eqs. (13)–(15) to obtain an analytic dependence of the order parameter R on coupling strength ε and phase shift α. The disadvantage of this representation is that by choosing values of A and Ω, we cannot predict to which phase shift α these values correspond. To have a dependence $R(\varepsilon)$ at a prescribed value of the phase shift α like one depicted in Fig. 1, we for each value of A considered many different values of Ω, calculated corresponding phase shifts, and determined the proper Ω via a one-dimensional root search algorithm. In this way, Fig. 1 was created.

C. Critical coupling: limit of vanishing amplitude A

Let us look at the limit $A \to 0$; this, according to Eq. (13), corresponds to $R = 0$, thus to the critical coupling ε_c. In this limit, it is convenient to consider representations (31) and (33).

For small $A \to 0$, we obtain from Eq. (31),

$$f_r(\Omega, 0) = \lim_{A\to 0}\frac{1}{2}\left[G_r\left(\frac{A}{1-\Omega}\right) - G_r\left(\frac{A}{-1-\Omega}\right)\right] = \begin{cases} \frac{\pi}{4}, & |\Omega| < 1, \\ 0, & |\Omega| > 1. \end{cases} \tag{35}$$

For the imaginary part, we obtain from Eq. (33) for $A \to 0$,

$$f_i(\Omega, 0) = \lim_{A\to 0}\frac{1}{2}\left[G_i\left(\frac{A}{1-\Omega}\right) - G_i\left(\frac{A}{-1-\Omega}\right)\right] = \frac{1}{4}\ln\left|\frac{1-\Omega}{1+\Omega}\right|. \tag{36}$$

Functions $f_i(\Omega, 0)$ and $f_r(\Omega, 0)$ yield the critical line on the (ε, α) plane. Because according to Eqs. (14) and (15),

$$\varepsilon_c^2 = \frac{1}{f_i^2 + f_r^2}, \quad \alpha = \arg(f_r + i f_i), \tag{37}$$

we obtain an explicit expression for the critical coupling

$$\varepsilon_c^2 = \frac{1}{f_r^2}\frac{1}{1+\tan^2\alpha} = \frac{16\cos^2\alpha}{\pi^2} \quad \Rightarrow \quad \varepsilon_c = \frac{4}{\pi}\cos\alpha. \tag{38}$$

We stress that because $f_r \geqslant 0$, the possible range of values of parameter α is $-\pi/2 < \alpha < \pi/2$. In this range, the coupling is attractive, while for $\alpha > \pi/2$ and $\alpha < -\pi/2$ the coupling is repulsive and there is no synchronization transition.

A remarkable property of expression (38) is that the synchronization threshold is maximal for maximal attraction $\alpha = 0$ and vanishes for neutral (conservative) coupling $\alpha = \pm\pi/2$. This is in contrast to the critical coupling behavior for other typical distributions of the frequencies $g(\omega)$ considered in the literature. For example, for the Cauchy distribution of natural frequencies, the critical coupling strength is *inversely* proportional to $\cos\alpha$ and tends to infinity in the conservative limit.

D. Small amplitudes A

As it follows from Eq. (36), the case $\pi/2 > \alpha > 0$ corresponds to $\infty > f_i > 0$ and thus to $-1 < \Omega < 0$ at $A = 0$. Without loss of generality, we consider negative values of parameter Ω also for $A > 0$ (the case of negative α corresponds to the symmetric case of positive frequencies Ω). To simplify the analysis below, we define $\delta = 1 + \Omega$, $\delta \leqslant 1$. In Eqs. (35) and (36), enter values

$$\frac{A}{-1-\Omega} = -\frac{A}{\delta} = Y_-, \quad \frac{A}{1-\Omega} = \frac{A}{2-\delta} = Y_+.$$

The regions of different values of Y_-, Y_+ depending on A, δ are depicted in Fig. 5. In these notations, quantity Q [from Eq. (24)] is represented as

$$Q = \begin{cases} 1, & A > 2-\delta, \\ \frac{A+\delta}{2}, & \delta \leqslant A \leqslant 2-\delta, \\ A, & A < \delta. \end{cases} \tag{39}$$

These values are also depicted in Fig. 5.

Here, we consider small values of A, so that $0 \leqslant A \lesssim 1$, $\delta \leqslant 1$. In terms of the variables Y_- and Y_+, we rewrite Eq. (34) as

$$f(\Omega, A) = \tfrac{1}{2}\,[G_r(Y_+) - G_r(Y_-)] + i\tfrac{1}{2}[G_i(Y_+) - G_i(Y_-)]. \tag{40}$$

For small A, we have $0 \leqslant Y_+ \leqslant 1$, while with regard to Y_- we have two domains:

$$\begin{array}{ll} -1 < Y_- < 0, & \text{for } A < \delta, \\ Y_- < -1, & \text{for } A > \delta. \end{array}$$

Thus, the function $f = f_r + i f_i$ has two representations in these domains.

For $A < \delta$,

$$f_r(\Omega, A) = F_r(Y_-, Y_+) = \frac{\pi}{4} f_i(\Omega, A) = F_i(Y_-, Y_+) = \frac{1}{4}\frac{1}{1+\sqrt{1-Y_+^2}} + \frac{1}{8}\ln(2 + 2\sqrt{1-Y_+^2} - Y_+^2)$$

$$- \frac{1}{4}\ln|Y_+| - \frac{1}{4}\frac{1}{1+\sqrt{1-Y_-^2}} - \frac{1}{8}\ln(2 + 2\sqrt{1-Y_-^2} - Y_-^2) + \frac{1}{4}\ln|Y_-|. \tag{41}$$

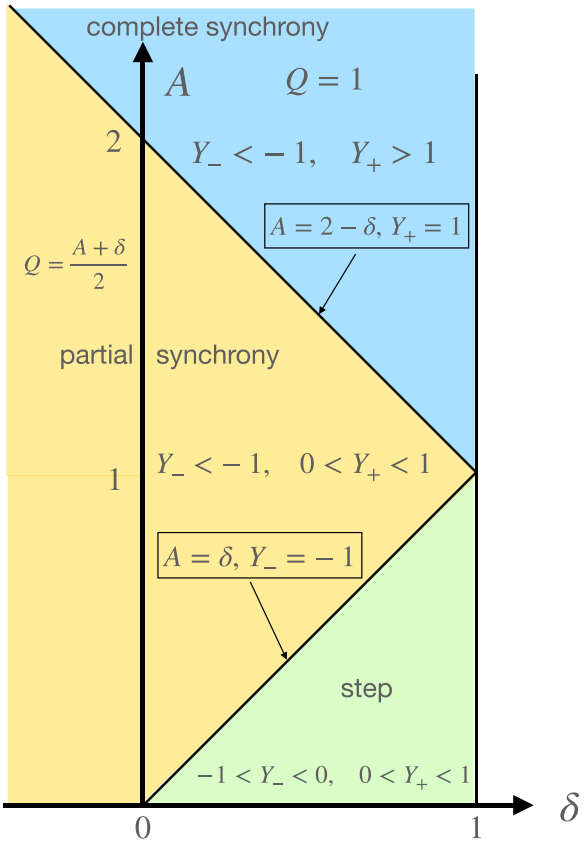


FIG. 5. Regions of different regimes on the (A, δ) plane and the corresponding values of $Y_{\pm}$, Q. The fraction of locked oscillators grows with A continuously up to line $A = 2 - \delta$, on which this fraction achieves its maximum possible value $Q = 1$ and does not grow anymore. The range with $A < \delta$ is mapped to a single value of the coupling ε_c; thus, the continuous growth with parameter A is observed as a step in the ε dependence of the order parameters R and Q. The domain $\delta < A < 2 - \delta$ corresponds to a continuous growth of R, Q with ε as illustrated in Fig. 1.

For $A > \delta$,

$$f_r(\Omega, A) = F_r(Y_-, Y_+) = \frac{\pi}{8} - \frac{1}{4}(\arcsin(Y_-^{-1}) + Y_-^{-1}\sqrt{1 - Y_-^{-2}})$$
$$f_i(\Omega, A) = F_i(Y_-, Y_+) = \frac{1}{2}\left[\frac{1}{2}\frac{1}{1 + \sqrt{1 - Y_+^2}} + \frac{1}{4}\ln(2 + 2\sqrt{1 - Y_+^2} - Y_+^2) - \frac{1}{2}\ln|Y_+|\right] - \frac{1}{4}\frac{1}{Y_-^2}. \tag{42}$$

Expressions (41) and (42) allow for the analysis of the transition to synchrony at ε_c.

In the domain $A < \delta$, because $f_r = \text{const} = \pi/4$, the value of $f_i = f_r \tan\alpha$ is also constant for fixed α. Thus, in this domain $\varepsilon = \text{const}$, while A varies from 0 at $Y_- = 0$ to δ at $Y_- = -1$. This domain corresponds to a step in the R versus ε dependence and is correspondingly marked in Fig. 5.

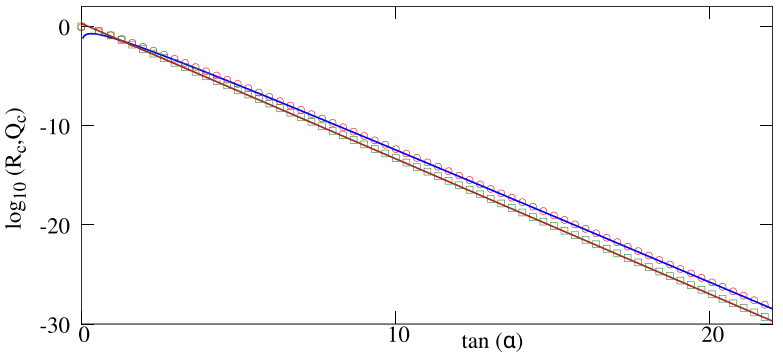


FIG. 6. Parameters of the discontinuous transition, R_c and Q_c, as functions of α. The values of R_c and Q_c according to exact expressions (43) are shown with red circles and green squares, respectively. The blue and the brown lines show approximate expressions (44).

If $Y_- = -1$, then $Y_+ = \frac{\delta}{2-\delta}$. Thus, the step amplitude R is determined in parametric form ($0 < \delta < 1$ is the parameter) from the equations

$$\frac{\pi}{4}\tan\alpha = F_i\left(-1, \frac{\delta}{2-\delta}\right) = \frac{1}{4}\left(\frac{1}{1+\sqrt{1-\delta^2/(2-\delta)^2}} - 1\right) + \frac{1}{8}\ln(2 + 2\sqrt{1-\delta^2/(2-\delta)^2} - \delta^2/(2-\delta)^2) - \frac{1}{4}\ln\frac{\delta}{2-\delta},$$

$$R_c = \delta\sqrt{(\pi/4)^2 + F_i^2\left(-1, \frac{\delta}{2-\delta}\right)}, \quad Q_c = \delta. \tag{43}$$

Here, we added the value of Q that follows from Eq. (39). Expression (43) gives the value of the steps R_c and Q_c as functions of phase shift α, in a parametric form. Figure 3 is drawn using this formula.

Let us look at the limit $\alpha \approx \pi/2$. It corresponds to $0 < \delta \ll 1$. In this limit, the main contribution to F_i is from the last logarithm term: $F_i \approx -\frac{1}{4}\ln(\delta/2) \gg 1$. This allows for representing $\delta \approx 2\exp(-\pi\tan\alpha)$ so that

$$R_c \approx \frac{\pi}{2}\exp(-\pi\tan\alpha)\tan\alpha, \quad Q_c \approx 2\exp(-\pi\tan\alpha). \tag{44}$$

Figure 6 shows the steps in R and Q as functions of α and the comparison to the approximate formula (44). Remarkably, the steps remain finite in the whole range of parameter α, albeit for α close to $\pi/2$ they are exponentially small.

E. Transition to complete synchrony

At complete synchrony, all oscillators are locked and $Q = 1$. This happens, according to expression (39), on the line $A = 2 - \delta$ (see Fig. 5). At these values of A and δ, we have $Y_+ = 1$ and $Y_- = \frac{\delta-2}{\delta}$. Thus, according to general expressions (31), (33), and (34), we have

$$G_r(Y_+) = \frac{\pi}{4}, \quad G_i(Y_+) = \frac{1}{2},$$

$$G_r(Y_-) = \frac{1}{2}\arcsin(1/Y_-) + \frac{1}{2}\frac{\sqrt{1-(1/Y_-)^2}}{Y_-}$$

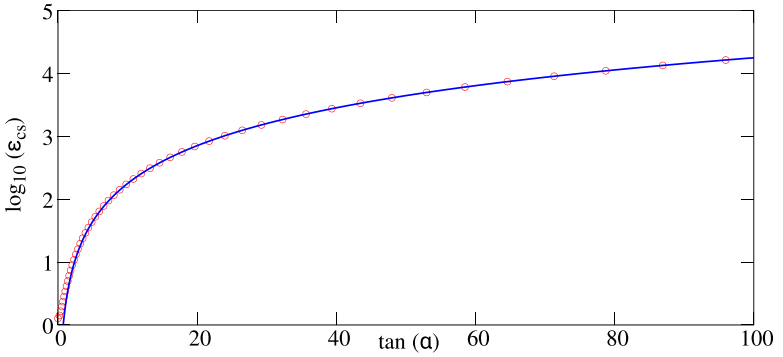


FIG. 7. Comparison of the exact values of ε_{cs} calculated according to Eq. (45) (circles) with the asymptotic at $\alpha \to \pi/2$ expression (46) (blue line).

$$= \frac{1}{2}\arcsin\frac{\delta}{\delta-2} - \sqrt{1-\delta}\,\frac{\delta}{(\delta-2)^2},$$

$$G_i(Y_-) = \frac{\delta^2}{2(\delta-2)^2},$$

$$f_r^{cs} = \frac{1}{2}\left(\pi/4 - \frac{1}{2}\arcsin\frac{\delta}{\delta-2} + \sqrt{1-\delta}\,\frac{\delta}{(\delta-2)^2}\right),$$

$$f_i^{cs} = \frac{1}{2}\left(\frac{1}{2} - \frac{\delta^2}{2(\delta-2)^2}\right) = \frac{1-\delta}{(\delta-2)^2}.$$

According to these expressions, the border of complete synchrony ε_{cs} as a function of α is given parametrically:

$$\alpha = \arg\left(f_r^{cs}(\delta) + i f_i^{cs}(\delta)\right), \quad \varepsilon_{cs} = \frac{1}{\sqrt{\left(f_r^{cs}\right)^2(\delta) + \left(f_i^{cs}\right)^2(\delta)}},$$

$$R_{cs} = A/\varepsilon = (2-\delta)\sqrt{\left(f_r^{cs}\right)^2(\delta) + \left(f_i^{cs}\right)^2(\delta)}. \tag{45}$$

These expressions are used to draw the curve $\varepsilon_{cs}(\alpha)$ in Fig. 7.

Next, we explore the rate of divergence of the value of ε_{cs} at $\alpha \to \pi/2$. To take limit of large negative δ where $\alpha \to \pi/2$, it is more convenient to represent f_r via expressions (34) [using $X_+ = 1/Y_+ = 1$ and $X_- = 1/Y_- = \delta/(\delta-2)$]:

$$f_r^{cs} = \frac{1}{2}[H_r(X_+) - H_r(X_-)] = \frac{1}{2}\int_{\delta/(2-\delta)}^{1}\sqrt{1-x^2}\,dx \approx \frac{4}{3}(2-\delta)^{-3/2}.$$

For $\delta \to \infty$, we have $f_r^{cs} \approx \frac{4}{3}|\delta|^{-3/2}$ and $f_i^{cs} \approx \delta^{-1}$. Thus, $\tan\alpha = f_i^{cs}/f_r^{cs} \approx \frac{3}{4}|\delta|^{1/2}$ and

$$\varepsilon_{cs} \approx |\delta| \approx \tfrac{16}{9}\tan^2\alpha. \tag{46}$$

In Fig. 7, we compare the exact value of threshold of the complete synchrony ε_{cs} versus α according to Eq. (45) with the approximation (46).

V. STABILITY

The theoretical analysis above yields a solution for the self-consistent synchronized state in the thermodynamic limit, and it should generally be supplemented with stability considerations.

Stability analysis should generally include time-dependent perturbations to the stationary density $\rho(\varphi|\omega)$, which constitutes a highly nontrivial mathematical problem. In Ref. [21], a simplified approach has been followed: It was assumed that at each frequency ω, the time-dependent density $\rho(\varphi, t|\omega)$ is a wrapped Cauchy distribution characterized by one complex variable $z(\omega, t)$, and the stability was analyzed within this subspace of perturbations (this subspace is an invariant Ott-Antonsen manifold). Consideration of stability of the asynchronous state [a uniform distribution $\rho(\varphi|\omega)$] gave the stability threshold ε_c, which coincides with the condition for the onset of the nontrivial self-consistent solutions (37) and (38) (see Sec. 4.1 of Ref. [21]). Thus, for $\varepsilon > \varepsilon_c$ the asynchronous state is unstable. Furthermore, in Ref. [21] it was demonstrated that a nontrivial solution can change its stability only via a fold bifurcation, i.e., if the solution has several branches. In our case of uniform distribution of frequencies, there is only one branch and thus the nontrivial self-consistent solution is stable in the whole range $\varepsilon > \varepsilon_c$. Because multistability is not possible, we conclude that all the transitions occur without hysteresis. We stress that although it is believed that the reduction to the Ott-Antonsen manifold does not affect stability conditions, formally the analysis in the full space of distributions is needed (see Refs. [5,15], where, in particular, the Kuramoto model with a uniform distribution of frequencies is treated). Stability of the nontrivial solution is confirmed by direct numerical simulations presented in Fig. 1. One can see that the discontinuous transition to synchrony is quite well reproduced in the finite ensemble. However, for α close to $\pi/2$, where the step becomes very small, there is no possibility to observe a step due to relatively large fluctuations of the order parameter $\sim N^{-1/2}$.

VI. QUALITATIVE INTERPRETATION AND GENERALIZATIONS

A uniform distribution of frequencies (19) is a special case. Although it allows for a complete analytical description in the thermodynamic limit as described above, a natural question is whether the found qualitative properties are specific to the uniform distribution case or can be generalized for other distributions. Let us formulate these properties:

(1) Transition to (partial) synchrony is discontinuous.
(2) There is a second transition to complete synchrony.
(3) The transition threshold decreases with phase shift parameter α.
(4) The transition threshold vanishes in the limit of neutral coupling $\alpha = \pm\pi/2$.

Below, we discuss these properties, striving to remain as analytical as possible. We rely on the exact analytical expressions in the form of integrals (valid for any distribution) presented in Sec. III A, and will see that in some cases, representation of these integrals in terms of elementary and special functions is possible for deviations from the uniform distribution.

A. Discontinuous versus continuous transition

Discontinuity of the transition for a uniform distribution is clearly related to a degenerate flat maximum of this distribution. A nondegenerate smooth maximum leads to a continuous transition, as has been demonstrated for the Kuramoto model in Refs. [2,3], and for the Kuramoto-Sakaguchi model in Ref. [21]. To illustrate this, we consider the Kuramoto case explored in Ref. [11], with a distribution having a nondegenerate maximum at zero:

$$g(\omega) = \begin{cases} \frac{1}{2} + \gamma \cos \pi\omega, & |\omega| < 1, \\ 0, & |\omega| > 1. \end{cases} \tag{47}$$

For this distribution, the integral (18) can be calculated explicitly for $A < 1$:

$$f(0, A) = \frac{\pi}{4} + \gamma A^{-1} J_1(\pi A), \tag{48}$$

where J_1 is the Bessel function of the first kind. Substitution of this function in Eq. (22) yields the dependence of the order parameter R on the coupling constant ε at small values of the order

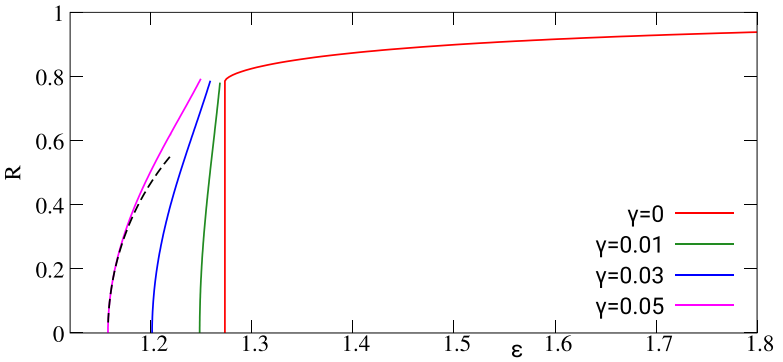


FIG. 8. Order parameter R vs ε for several values of γ. Dashed black line: approximate expression (49).

parameter, as illustrated in Fig. 8. One can see that the transition to synchrony is now continuous. Furthermore, close to the transition point where $A = 0$, one can approximate the Bessel function as $J_1(x) \approx x/2 - x^3/16$. With this approximation, the dependence of the order parameter on the coupling strength can be represented explicitly:

$$R = \frac{4}{\pi\varepsilon}\sqrt{\frac{\pi/4 + \gamma\pi/2 - 1/\varepsilon}{\pi g}}, \quad \varepsilon \geqslant \frac{4}{\pi + 2\pi\gamma}. \tag{49}$$

This approximate expression is compared with an exact one in Fig. 8 for $\gamma = 0.05$.

B. Transition to complete synchrony

This property is just related to the compactness of the distribution $g(\omega)$: In the case of infinite tails, there are always oscillators outside of the synchronization region (Arnold tongue) of the mean-field driving, which are not locked. We note here that in finite-size simulations, the transition to complete synchrony also occurs for unbounded distributions.

C. Synchronization threshold and its dependence on the phase shift parameter

To understand dependence of the synchronization threshold on α, it is instructive to rewrite the self-consistency condition (9) as

$$Ae^{i\alpha} = \varepsilon A f(\Omega, A), \tag{50}$$

and to interprete Eq. (50) as the balance of the amplitude and of the phase of the mean-field driving. A natural interpretation of the function $f(\Omega, A)$ is a nonlinear response function for driving at frequency Ω with amplitude A. For the synchronization threshold, the linear response function $f(\Omega, 0)$ is essential, because this threshold is determined from the linearized condition

$$e^{i\alpha} = \varepsilon_c f(\Omega, 0). \tag{51}$$

Linear response can be obtained by taking a (nontrivial) limit $A \to 0$ in Eq. (11), which, as has been demonstrated in Ref. [21], reads

$$f(\Omega, 0) = \frac{\pi}{2}(g(\Omega) - i\hat{H}[g(\Omega)]), \quad \hat{H}[g(\Omega)] = \frac{1}{\pi}\text{P.V.}\int \frac{g(x)}{\Omega - x}dx. \tag{52}$$

Here, $\hat{H}$ is the Hilbert transform operator. Expression (52) is nothing else but the Kramers-Kronig relation [22,23]. To understand the physical meaning of two terms in the linear response function, let us consider a very small but finite A, taking into account the densities of oscillators according to Eq. (7). Then, the oscillators close in frequency to the driving value Ω are locked and have (on

average) the same phase as the driving force; this contributes to the real part of the response function, proportionally to their number $g(\Omega)$. The nonlocked oscillators rotate, and on average their field is shifted by $\pm\pi/2$ to the driving force; thus, all these oscillators contribute to the imaginary part of the response function, and the sum of these contributions is expressed by the Hilbert transform integral in Eq. (52). For further consideration, let us suppose that the distribution $g(\Omega)$ is even. Then, the imaginary part of the response function is odd and vanishes at $\Omega = 0$. This value solves Eq. (51) in the Kuramoto case $\alpha = 0$, yielding well-known result $\varepsilon_c = \frac{2}{\pi} g(0)$. On the other hand, for a nonzero phase shift α, i.e., in the Kuramoto-Sakaguchi case, the imaginary part of the response function should be nonzero, to match the argument of the left-hand side of Eq. (51). To see whether the critical coupling ε_c grows or decreases with parameter α, we need to know how the absolute value of the response function varies with Ω. Generally, the real part decreases, and the imaginary part grows with $|\Omega|$, but it is difficult *a priori* to conclude which of the effects generally prevails. However, this is clear for the uniform distribution: Here, the real part $g(\Omega)$ is constant, so that $|f(\Omega, 0)| < f(0, 0)$, which means that the critical coupling decreases with α. Physically, the total response includes contributions from locked and unlocked oscillators, and the latter becomes more important for larger values of the phase shift in the coupling, because only unlocked oscillators provide a proper argument of the response function. Thus, the effective force increases, and therefore the critical coupling is smaller. We expect this to be valid also for rather flat distributions, while for peaked distributions, the decrease of $g(\Omega)$ can be stronger than the increase of $\hat{H}[g(\Omega)]$, and the critical coupling increases with α.

To illustrate these qualitative considerations, we next consider several distributions whose Hilbert transforms can be calculated analytically (cf. Ref. [24]). The simplest example is a Cauchy distribution:

$$g(\Omega) = \frac{1}{\pi} \frac{1}{1+\Omega^2}, \quad \hat{H}[g(\Omega)] = \frac{1}{\pi} \frac{\Omega}{1+\Omega^2}. \tag{53}$$

This yields

$$f(\Omega, 0) = \frac{1}{2} \frac{1 - i\Omega}{1+\Omega^2} = \frac{\cos\alpha}{2} e^{i\alpha}, \quad \alpha = -\arctan\Omega, \tag{54}$$

and a well-known result $\varepsilon_c = 2/\cos\alpha$; here, the critical coupling grows with α. The next example is a triangular distribution

$$g(\Omega) = \begin{cases} 1 - |\Omega|, & |\Omega| < 1, \\ 0, & |\Omega| > 1, \end{cases} \quad \hat{H}[g(\Omega)] = -\frac{1}{\pi}\left[\ln\left|\frac{\Omega-1}{\Omega+1}\right| + \Omega \ln\left|\frac{\Omega^2}{\Omega^2-1}\right|\right], \tag{55}$$

which provides ε_c versus α dependence in a parametric form (see Fig. 9). Also, at least three cases of a symmetric Beta distribution

$$g(\Omega) = \begin{cases} C_a(1-x^2)^{a-1}, & |\Omega| < 1, \\ 0, & |\Omega| > 1, \end{cases} \quad C_a = \frac{\Gamma(2a)}{\Gamma^2(a) 2^{2a-1}} \tag{56}$$

allow for analytical results. The case $a = 1$ is the uniform distribution treated above. In the case $a = 2$, we have

$$g(\Omega) = \begin{cases} \frac{3}{4}(1-\Omega^2), & |\Omega| < 1, \\ 0, & |\Omega| > 1, \end{cases} \quad \hat{H}[g(\Omega)] = -\frac{3}{4\pi}\left[(1-\Omega^2)\ln\left|\frac{\Omega-1}{\Omega+1}\right| - 2\Omega\right]. \tag{57}$$

Here, similar to the triangular distribution, the critical coupling grows with α (see Fig. 9). In the case $a = 1.5$, we have

$$g(\Omega) = \begin{cases} \frac{2}{\pi}(1-\Omega^2)^{1/2}, & |\Omega| < 1, \\ 0, & |\Omega| > 1, \end{cases} \quad \hat{H}[g(\Omega)] = \frac{2}{\pi}\Omega. \tag{58}$$

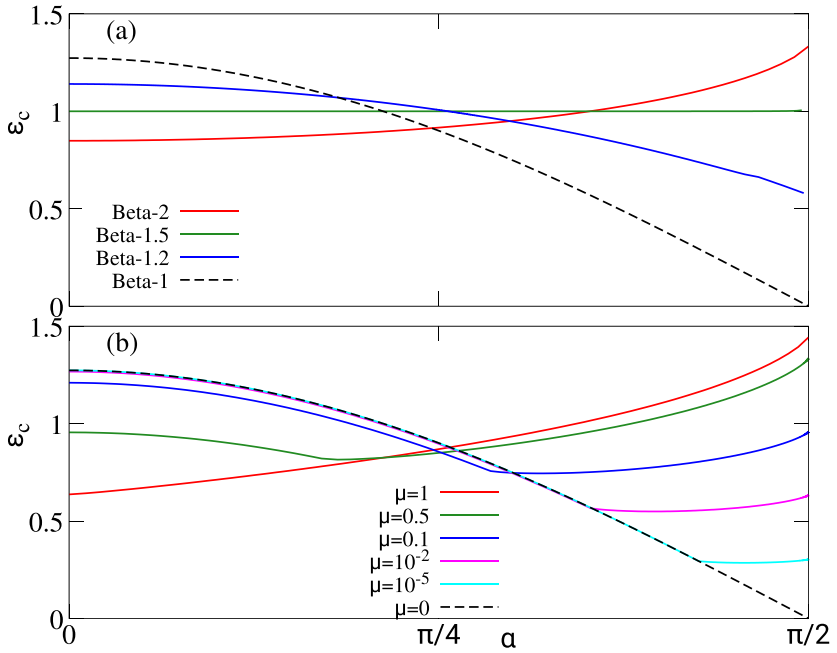


FIG. 9. Critical coupling ε_c vs phase shift parameter α. (a) Four cases of the Beta distribution (56), including the uniform distribution ($a = 1$). (b) For trapezoid distributions (59) with different values of parameter μ, including a triangular $\mu = 1$ and a uniform distribution ($\mu = 0$).

One can easily check that here $\varepsilon_c = 1$ independently of α. This is a borderline case, where the decrease of the real part of the response function is exactly compensated by the increase of the imaginary part. We expect that for $a < 1$, the symmetric Beta distribution has properties similar to that of the uniform distribution, i.e., decrease of the critical coupling with α. Unfortunately, we have not found an analytically solvable case in this range; therefore, for $a = 1.2$, we calculated the Hilbert transform numerically (see Fig. 9). Another case where one can interpolate between peaked and uniform distributions, and the Hilbert transform is available analytically, is a trapezoid distribution:

$$g(\Omega) = \begin{cases} \frac{1}{2-\mu}, & |\Omega| < 1-\mu, \\ \frac{1}{(2-\mu)(1-\mu)}(1-|\Omega|), & 1-\mu \leqslant |\Omega| \leqslant 1, \\ 0, & |\Omega| > 1, \end{cases}$$

$$\hat{H}[g(\Omega)] = -\frac{1}{\pi(2-\mu)}\left(\mu^{-1}\ln\left|\frac{(1-\mu+\Omega)(1-\Omega)}{(1-\mu-\Omega)(1+\Omega)}\right| + \mu^{-1}\Omega\ln\left|\frac{(1-\mu)^2-\Omega^2}{1-\Omega^2}\right| + \ln\left|\frac{1-\mu-\Omega}{1-\mu+\Omega}\right|\right). \tag{59}$$

The case $\mu = 1$ is a triangular distribution (55), while a uniform distribution (19) corresponds to $\mu = 0$. We present the critical coupling for several values of μ in Fig. 9(b). For $\mu = 0, 1$, the dependence of ε_c on α is monotonic, but between these limiting cases it is nonmonotonic.

Finally, let us discuss, on the basis of the response function expression (52), in which cases the critical coupling ε_c can vanish. This can happen if $f(\Omega, 0)$ diverges at some values of Ω. Because we consider nonsingluar distributions $g(\Omega)$, the only source of singularity is the imaginary part $\hat{H}[g(\Omega)]$. Thus, at the singularity $\alpha = \arg(f(\Omega, 0)) = \pm\pi/2$ and the critical coupling can vanish

only at $\alpha = \pm\pi/2$, i.e., for a neutral interaction of oscillators. The source of possible divergence is the singularity $\sim(\Omega - x)^{-1}$ in the Hilbert transform (52). Because of the principal value in this transform, for a smooth $g(\Omega)$, the Hilbert transform remains finite due to cancellation of contributions with $\Omega \pm x$ for small x to the integral (52). However, if $g(\Omega)$ possesses a step, then at the position of the step, there is no cancellation and a logarithmic singularity in $\hat{H}[g(\Omega)]$ appears [cf. expression (36) with logarithmic singularities at $\Omega = \pm 1$]. Thus, vanishing critical coupling is possible only for distributions possessing steps, and any smoothing of a step leads to nonzero values of ε_c (cf. the curve in Fig. 9 for a Beta distribution with $a = 1.2$). Physically, for a distribution with a step, the balance of the contributions to the response function from the unlocked oscillators having phase shifts $\pm\pi/2$ with respect to the force is violated, and the response close to the border frequency becomes very large. One can say that the ensemble is extremely sensitive to the forcing at frequencies where there are many more oscillators on one side of the Arnold tongue than on another, and a collective mode appears already for very small coupling.

VII. CONCLUSIONS

In this paper, we presented an analytic theory of the synchronization transition in the Kuramoto-Sakaguchi model of coupled phase oscillators, for a uniform distribution of natural frequencies. Because the distribution has a finite support, two essential transitions can be identified: (1) First, at ε_c, a discontinuous transition from disorder to partial synchrony happens, at which a fraction of oscillators becomes synchronized (mutually and with the mean field), while other units are not locked. (2) The second transition at $\varepsilon_{cs} \geqslant \varepsilon_c$ is from the partially synchronous state to complete synchrony, at which all oscillators are locked to the mean field. This second transition does not occur if the frequency distribution has infinite support (such as a Gaussian or Cauchy distribution).

The two critical coupling strengths depend on the phase shift in the coupling. They coincide at the vanishing phase shift (Kuramoto model), so there is just one transition from disorder to complete synchrony. Remarkably, the first critical coupling ε_c *decreases* with the phase shift and tends to zero as the coupling becomes conservative at $\alpha = \pm\pi/2$. This property is in contradistinction to a popular case of a Cauchy distribution of frequencies, where the critical coupling *increases* when the coupling becomes less attractive. Notably, although the critical coupling for α close to $\pm\pi/2$ is small, the appearing synchrony is very weak because the discontinuous step of the order parameter is exponentially small in this limit. Moreover, the range of partial synchrony also diverges close to the neutral coupling, and the second critical value ε_{cs} diverges $\sim \tan^2\alpha$ in this limit. We have argued, based on the representation of the linear response function as an analytic signal, that a decrease of the critical coupling with α is related to a relative flatness of the distribution of the frequencies, and is present also for smooth distributions. However, for the critical coupling to vanish (which can happen for neutral interaction with $\alpha = \pm\pi/2$ only), steps in the distribution density are essential. Discontinuity of the transition disappears if the maximum of the distribution density becomes nondegenerate. On the other hand, a transition to complete synchrony appears to be common for distributions with a compact support. Finally, we mention that our consideration is restricted to the thermodynamic limit; for finite-size effects, see Refs. [11,14,25,26].

ACKNOWLEDGMENT

The author thanks F. Bagnoli and S. Iubini for fruitful discussions.

DATA AVAILABILITY

The data that support the findings of this article are not publicly available upon publication because it is not technically feasible and/or the cost of preparing, depositing, and hosting the data would be prohibitive within the terms of this research project. The data are available from the authors upon reasonable request.

[1] S. Gupta, A. Campa, and S. Ruffo, *Statistical Physics of Synchronization* (Springer, Cham, Switzerland, 2018).
[2] Y. Kuramoto, Self-entrainment of a population of coupled nonlinear oscillators, in *International Symposium on Mathematical Problems in Theoretical Physics*, edited by H. Araki, Lecture Notes in Physics (Springer, New York, 1975), Vol. 39, p. 420.
[3] Y. Kuramoto, *Chemical Oscillations, Waves and Turbulence* (Springer, Berlin, 1984).
[4] J. A. Acebrón, L. L. Bonilla, C. J. P. Vicente, F. Ritort, and R. Spigler, The Kuramoto model: A simple paradigm for synchronization phenomena, Rev. Mod. Phys. **77**, 137 (2005).
[5] H. Dietert, Stability and bifurcation for the Kuramoto model, J. Math. Pures Appl. **105**, 451 (2016).
[6] I. Z. Kiss, Y. Zhai, and J. L. Hudson, Emerging coherence in a population of chemical oscillators, Science **296**, 1676 (2002).
[7] A. A. Temirbayev, Y. D. Nalibayev, Z. Z. Zhanabaev, V. I. Ponomarenko, and M. Rosenblum, Autonomous and forced dynamics of oscillator ensembles with global nonlinear coupling: An experimental study, Phys. Rev. E **87**, 062917 (2013).
[8] H. Daido, Onset of cooperative entrainment in limit-cycle oscillators with uniform all-to-all interactions: Bifurcation of the order function, Physica D **91**, 24 (1996).
[9] H. Chiba and I. Nishikawa, Center manifold reduction for large populations of globally coupled phase oscillators, Chaos **21**, 043103 (2011).
[10] M. Komarov and A. Pikovsky, The Kuramoto model of coupled oscillators with a bi-harmonic coupling function, Physica D **289**, 18 (2014).
[11] D. Pazó, Thermodynamic limit of the first-order phase transition in the Kuramoto model, Phys. Rev. E **72**, 046211 (2005).
[12] A. Ghosh and S. Gupta, Relaxation dynamics of the Kuramoto model with uniformly distributed natural frequencies, Physica A **392**, 3812 (2013).
[13] D. Yuan and J.-Z. Yang, Conformists and contrarians in a Kuramoto model with uniformly distributed natural frequencies, Commun. Theor. Phys. **59**, 684 (2013).
[14] B. Ottino-Löffler and S. H. Strogatz, Kuramoto model with uniformly spaced frequencies: Finite-N asymptotics of the locking threshold, Phys. Rev. E **93**, 062220 (2016).
[15] J. Bramburger and M. Holzer, Capturing the critical coupling of large random Kuramoto networks with graphons, arXiv:2503.01589.
[16] H. Sakaguchi and Y. Kuramoto, A soluble active rotator model showing phase transition via mutual entrainment, Prog. Theor. Phys. **76**, 576 (1986).
[17] E. Ott and T. M. Antonsen, Low dimensional behavior of large systems of globally coupled oscillators, Chaos **18**, 037113 (2008).
[18] K. Wiesenfeld, P. Colet, and S. H. Strogatz, Frequency locking in Josephson arrays: Connection with the Kuramoto model, Phys. Rev. E **57**, 1563 (1998).
[19] M. Kapitaniak, K. Czolczynski, P. Perlikowski, A. Stefanski, and T. Kapitaniak, Synchronization of clocks, Phys. Rep. **517**, 1 (2012).
[20] O. E. Omel'chenko and M. Wolfrum, Nonuniversal transitions to synchrony in the Sakaguchi-Kuramoto model, Phys. Rev. Lett. **109**, 164101 (2012).
[21] E. Omel'chenko and M. Wolfrum, Bifurcations in the Sakaguchi–Kuramoto model, Physica D **263**, 74 (2013).
[22] H. A. Kramers, La diffusion de la lumiére par les atomes, in *Atti del Congresso Internazionale dei Fisici*, Vol. 2 (The International Congress of Physics, Como, Italy, 1927), pp. 545–557.
[23] R. de L. Kronig, On the theory of dispersion of x-rays, J. Opt. Soc. Am. **12**, 547 (1926).
[24] S. L. Hahn, *Hilbert Transforms in Signal Processing*, 1st ed. (Artech House, Norwood, MA, 1996)
[25] S. Eydam and M. Wolfrum, Mode locking in systems of globally coupled phase oscillators, Phys. Rev. E **96**, 052205 (2017).
[26] T. Coletta, R. Delabays, and P. Jacquod, Finite-size scaling in the Kuramoto model, Phys. Rev. E **95**, 042207 (2017).